A simple method to clean ligand contamination on TEM grids

To cite the paper, please use this: C. Li et. al., Ultramicroscopy 221 (2021) 113195

A simple method to clean ligand contamination on TEM grids

Chen Li [a,*], Adrian Pedrazo Tardajos [a], Da Wang [a], Daniel Choukroun [b], Kevin Van Daele [b], Tom Breugelmans [b] & Sara Bals [a]

[a] Electron microscopy for Materials research (EMAT), University of Antwerp, Groenenborgerlaan 171, 2020 Antwerpen, Belgium

[b] Applied Electrochemistry & Catalysis (ELCAT), University of Antwerp, Universiteitsplein 1, 2610 Wilrijk, Belgium

* Corresponding author. E-mail address: lichen0320@gmail.com

Abstract:

Colloidal nanoparticles (NPs) including nanowires and nanosheets made by chemical methods involve many organic ligands. When the structure of NPs is investigated via transmission electron microscopy (TEM), the organic ligands act as a source for e-beam induced deposition and this causes substantial build-up of carbon layers in the investigated areas, which is typically referred to as "contamination" in the field of electron microscopy. This contamination is often more severe for scanning TEM, a technique that is based on a focused electron beam and hence higher electron dose rate. In this paper, we report a simple and effective method to clean drop-cast TEM grids that contain NPs with ligands. Using a combination of activated carbon and ethanol, this method effectively reduces the amount of ligands on TEM grids, and therefore greatly improves the quality of electron microscopy images and subsequent analytical measurements. This efficient and facile method can be helpful during electron microscopy investigation of different kinds of nanomaterials that suffer from ligand-induced contamination.

Keyword: Colloidal nanoparticles, TEM, contamination, ligands

1. Introduction

Nanoparticles (NPs) including nanowires and nanosheets show interesting optical, chemical, electrical, and physical properties that are very different from their bulk counterparts, and therefore play an important role in a wide range of fields. Very often, (organic) ligands are used to control the morphology and stability of the NPs as well as to modify their properties [1,2]. However, when the structure of these NPs is investigated by transmission electron microscopy (TEM), the incident electrons attract the organic ligands and break the bonds of the hydrocarbons, forming thick carbon layers in the area of interest. This phenomenon is often referred to as contamination in the field of electron microscopy [3,4]. The formation of such e-beam induced contamination is similar to e-beam induced deposition used as a lithography (EBL) technique, although for the latter a precursor gas is intentionally induced for deposition [5,6]. When colloidal NPs are drop-cast onto TEM grids, not only the ligands bonded with the NPs but also the ligands in the solution will leave residues on TEM grids and contribute to contamination. This contamination problem is more severe for scanning TEM (STEM), in which the electron beam is focused into a small probe and tends to have a high dose rate, forming e-beam induced contamination relatively rapidly. The illustrations in Fig. 1 demonstrate this

process. In general, the thickness of the contamination increases when the magnification and acquisition time increase [7]. The higher the magnification, the faster contamination builds up, which makes atomic-resolution imaging very challenging. Similar problems occur for analytical analyses such as electron energy loss spectroscopy (EELS) and energy-dispersive X-ray spectroscopy (EDX) that require long acquisition times.

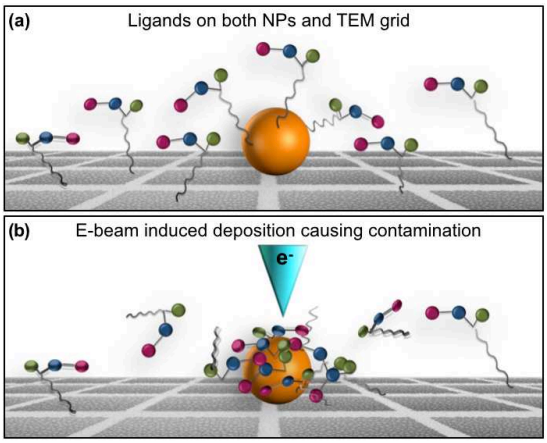

Figure 1. Schematic illustrations demonstrating how e-beam induced deposition causes contamination on a TEM grid, which contains colloidal NPs (orange spheres) surrounded by ligands (red-blue-green chains).

A broad range of methods for decontamination treatments of TEM grids have been proposed, including plasma cleaning (on PtNi and PbS NPs [7]; carbon films [7,8]; Si [7,9], InAs [10], $SrTiO_3$ [9] and stainless steel [9,11] foils), beam showering (on PtNi and PbS NPs [7]; carbon films [7]; Si [7] and SiN [12] foils), heating in vacuum or in different atmospheres (on PtNi and PbS NPs [7]; graphene [4] and carbon films [7,8]; NiO thin film [7]), baking with activated carbon (on graphene [13]), cooling (on PtNi NPs [7]; organic specimens [14]), exposure to ultraviolet light and ozone (on Au and Sn particles [15]; carbon nanotubes [15]; graphene and carbon film [16]; Li-polymer [16]) and etching by exposure to low-pressure gas atmospheres under e-beam irradiation (on graphene [17]). All methods have their own advantages and disadvantages, some of which are summarized in Table 1 and TEM grids drop-cast with CuAg colloidal NPs capped by tetradecylphosphonic acid (TDPA) are used as testing material. The main conclusions are:

(1) Plasma cleaning using O_2 successfully removed hydrocarbon contamination. However, for materials that might react with O_2, including CuAg NPs, this is not a good solution. This limitation similarly applies for ozone treatment. Plasma using Ar or H_2 without O_2 did not show a significant sign of contamination removal. Another problem is that when the time used for the plasma cleaning was too long, the carbon support on the TEM grids showed partial damage and bending.

(2) Beam showering (shining a large electron flux on the samples at low magnification in TEM mode) worked very effectively for removing the contamination, albeit only for the relatively small areas (μm scale) that the electron beam can cover. Moreover, the cleaning effect was restricted in time (~ 30 minutes), as ligands from the surrounding non-

showered contaminated area diffused back to the clean area. Finally, beam-damage occurred if the beam shower was carried out too long.

(3) Heating the TEM grids at 160 °C for 8 hours in vacuum (~ 10^{-2} Pa range) did not remove the contamination for CuAg colloidal NPs. However, this method was applied in previous research and has sufficiently cleaned airborne hydrocarbon contamination on TEM grids [18,19]. These different results are likely related to the stronger bonding between the organic ligands and the CuAg NPs as well as the TEM grids in comparison to the bonding between airborne hydrocarbon and TEM grids. Moreover, a major concern for the heat treatment is that it might cause structural and compositional changes (i.e. alloying) in the samples.

(4) Heating TEM grids inside activated carbon was originally developed to clean graphene [13]. However, heating the grids up to 200 °C for 3 hours was not sufficient to remove the ligand contamination for CuAg colloidal NPs. Again, a major concern is that heating might cause structural and compositional changes in the samples, especially as oxidation might occur while the samples are heated in air.

Different methods		Advantages	Disadvantages
Published methods	(1) Plasma cleaning	✓ Large area	• O_2 Plasma: sample might oxidize • Without O_2: weak cleaning effect • Might damage TEM grid
	(2) Beam showering	✓ Effective for ligands	• Only cleans relatively small areas • Only last for limited period • Might cause beam damage
	(3) Heating in vacuum	✓ Effective for airborne hydrocarbon ✓ Large area	• Weak cleaning effect for ligands • Structure/composition might change
	(4) Activated carbon + heating	✓ Effective for airborne hydrocarbon ✓ Large area	• Weak cleaning effect for ligands • Structure/composition might change • Might oxidize when heating in air
Inspiring method	Carbon black + ethanol	✓ Effective for ligands ✓ Large area ✓ No heating	• Thick carbon layers reduce signal-noise ratio
New method	Activated carbon + ethanol	✓ Effective for ligands ✓ Large area ✓ No heating ✓ Efficient and facile	• If NPs have too high density at grid, they might accumulate

Table 1. Comparison of advantages and disadvantages between published methods and the method proposed in this manuscript.

In summary, it is important and urgent to find a new method that can effectively remove organic ligand-induced contamination on nanomaterials, and meanwhile does not involve heating or induce oxidization. In this paper, we develop a new and facile method to clean TEM grids containing nanomaterials surrounded by ligands. Our results show that this method drastically removes excess ligands on the TEM grid, thereby enabling atomic resolution imaging and spectrum imaging. By comparing with control experiments, the mechanism behind the novel method is explained. We furthermore discuss the parameters that can be tuned for different situations and different material systems.

2. Materials and microscopy information

The colloidal CuAg NPs used in this paper were synthesized using a two-step procedure [20]. First, polycrystalline Cu cores were synthesized by reacting 0.6 mmol of $Cu(OAc)_2 \cdot H_2O$ in 10 ml of trioctylamine with 0.3 mmol of TDPA. The reaction mixture was heated to 100°C and degassed by multiple vacuum-argon filling cycles. Then, the mixture was heated at ~4°C/min to 180°C, held at that temperature for 30 minutes and then heated to 250°C, followed by an additional dwell time of 30 minutes. Afterwards, the mixture was left to cool down and transferred under a positive Ar pressure to an Ar glove box for purification. Second, 1 ml of a 1-3 mg/ml purified Cu NPs suspension in isoamylether was mixed together with a Ag-trifluoroacetate solution in isoamylether inside the glove box. The mixture was vortexed at room temperature for a duration of 2-5 hours and then purified. More details are provided in the supplementary materials. A similar procedure was used to synthesize CuSn NPs, after replacing the Ag- precursor with a Sn- precursor [21].

The as-synthesized CuAg particle suspensions were purified by 2-3 rounds of precipitation and redissolution method [22]. A volume ratio of 1.25:1 between the suspension and a mixture of 50% ethanol + 50% 2-propanol was employed for centrifugation, which took place at 5000 rpm for a duration of 5 min, followed by supernatant removal and re-dispersion in hexane. Finally, the solution was further diluted and drop-cast onto TEM grids coated with ultrathin (3 nm) carbon film.

The activated carbon ("charcoal activated for analysis, extra pure") was purchased from Merck KGaA, Germany. The granular size is about 1.5 mm. The bulk density is 150-440 kg/m^3.

A Thermo Fisher Scientific Osiris microscope was used for acquiring STEM annular dark-field (ADF) images at 200 kV. Two Thermo Fisher Scientific probe-corrected Titan microscopes were used for acquiring atomic-resolution STEM-ADF and spectrum imaging at 300 kV. A probe current of 50 pA was used for ADF imaging, and 150 pA was used for EELS spectrum imaging.

3. Cleaning method development

In our search for a cleaning method that is effective for cleaning ligands but does not involve heating or oxidization, we were inspired by the behavior of a sample containing CuSn NPs on carbon black. When the solution-based CuSn NPs were drop-cast onto TEM grids, a high level of contamination was observed during microscopy investigation (Fig. S1(a1-a2)). Then, to obtain a good conducting electrode for electrochemical measurements, the CuSn NPs were dispersed on carbon black and ethanol was used to wash the NPs in order to remove impurities [21]. After the mixture of carbon black and NPs was dried, we characterized the sample by TEM. Surprisingly, there was little contamination surrounding the CuSn NPs (Fig. S1(b1-b2)). Obviously, carbon black and ethanol play an important role in removing the ligand-induced contamination. The

disadvantage of this method is that the carbon black on TEM grids forms a thick support for the NPs, which reduces the signal to noise ratio for either atomic-resolution imaging or spectrum imaging (Fig. S1(b1-b2)). Nevertheless, this method encouraged us to find a proper combination of solvent and adsorbent to clean TEM grids. The disadvantage of thick carbon residues from carbon black can be overcome by using other adsorbents, for instance activated carbon yielding much larger grain sizes (mm scale) that were used in heating decontamination treatments [13].

The optimized method based on ethanol and activated carbon is very easy to apply in practice. Figure 2 (a-d) shows the four major steps in this method. First, activated carbon is placed into a container as shown in Fig. 2 (a). Then, ethanol is poured into the container until the activated carbon is completely covered (Fig. 2(b)). As shown in Fig. 2 (c), many bubbles rise up from the activated carbon to the surface of the ethanol (also see Supplementary movie 1). A drop-cast TEM grid containing colloidal NPs is rapidly inserted into the ethanol, letting the bubbles go through as well as around the grid. Depending on the type and the density of the ligands used for the NPs, the time for submerging the TEM grid can be adjusted from a few seconds to until the bubbling process stops (i.e. after about 10 minutes). When submerging the TEM grid for just a few seconds, one can simply hold it using a tweezer (Fig. 2 (d)). The entire process can be seen in Supplementary movie 2. If a longer submerging time is needed, a clamp stand can be used to hold the tweezer.

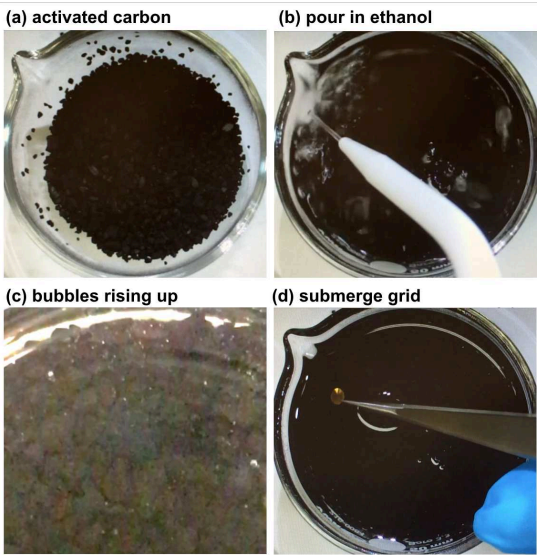

Figure 2 Step-by step demonstration of the new cleaning method. (a) Place activated carbon into a container, (b) pour ethanol into the container until all the activated carbon is covered, (c) a high density of bubbles rises up in the container (movie 1), then (d) a drop-cast TEM grid that contains colloid NPs is submerged into the ethanol. The spots with bright contrast in (c) are bubbles.

The comparison of contamination before and after this cleaning step shows a drastic difference, as demonstrated in Fig. 3. For the TEM grids (drop-cast with CuAg NPs) without the cleaning step, a rapid scan of 2.1 seconds on fresh areas was used to locate the area of interest (2 frames of imaging with a dwell time of 4 µs/pixel and a size of 512*512 pixels). Then, the magnification was reduced by a factor of two and then Fig. 3 (a1) was acquired (12.6 second scan with a dwell time of 12 µs/pixel and a size of

1024*1024 pixels). A bright contrast with a rectangular shape appeared at the middle of Fig. 3 (a1), which is a typical result from the build-up of carbon contamination at the scanned area. The higher the magnification and hence the higher the electron doses, the more severe this contamination problem becomes, behaving as the bright contrast around and on the NPs in Fig. 3 (a2) and (a3), and eventually preventing atomic resolution imaging. After applying the proposed cleaning method for two minutes, atomic resolution imaging of the CuAg NPs on the same TEM grid became feasible, as shown in Fig. 3 (b1-b2). Electron energy loss spectrum (EELS) imaging, using a probe current of 150 pA and acquisition time of 2 minutes also became possible (Fig. S2), with only slight contamination observed afterwards. This cleaning method was also applied to the CuSn NPs, and clearly reduced the contamination as shown in Fig. S1(c1-2).

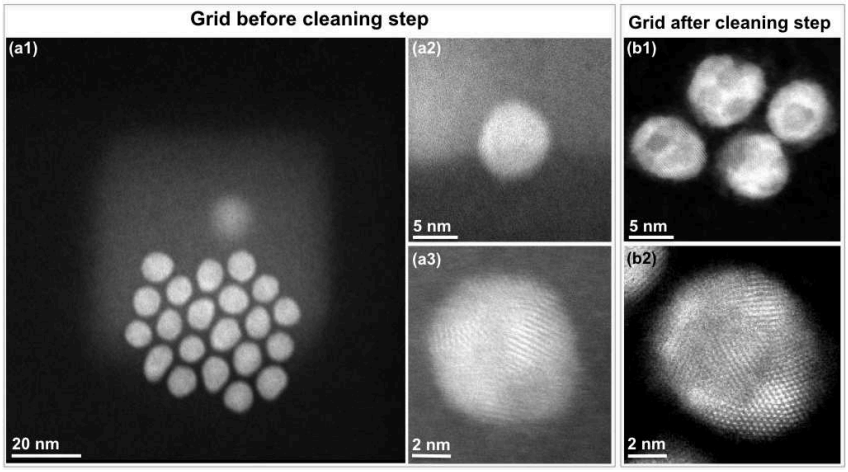

Figure 3 A comparison of the contamination situations before and after cleaning the TEM grid with CuAg NPs. (a1-a3) For the TEM grid before the cleaning step, a rapid scan of 2.1 seconds on fresh areas was used to locate the area of interest. Then the magnification was reduced by a factor of two and image (a1) was acquired. The bright contrast with the rectangular shape in the middle of image (a1) and the bright contrast around and on the NPs in (a2) and (a3) are typical results from the build-up of carbon contamination at the scanned areas. (b1-b2) For the TEM grid after the proposed cleaning step, there was no carbon layer contamination observed at the scanned areas, which allows much better contrast and image resolution.

When submerging the grids for longer periods after the appearance of bubbles ended (e.g. 2 and 24h), no further improvement in contamination reduction was found. Therefore, we assume that the period during which the bubbles appear is the most effective to clean the grids. If the grid is not cleaned sufficiently after being processed for the entire "bubbling" period, one can repeat the cleaning process using fresh activated carbon.

Alternatively, a more aggressive version of the cleaning method shown in Fig. 4 can be applied. Hereby, a TEM grid is placed on top of the activated carbon before the ethanol is poured into the container. The entire process is demonstrated in Supplementary movie 3. The disadvantage of this approach is that small residual carbon pieces might attach to the TEM grid, due to the direct contact with the activated carbon. However, for NPs consisting of heavy elements such as Cu and Ag, carbon contrast is not hampering STEM-ADF imaging, as shown in Fig. S3. On the other hand, for materials composed of light elements, such as carbon nanotubes or BN nanowires, direct contact between TEM grids and activated carbon should be avoided.

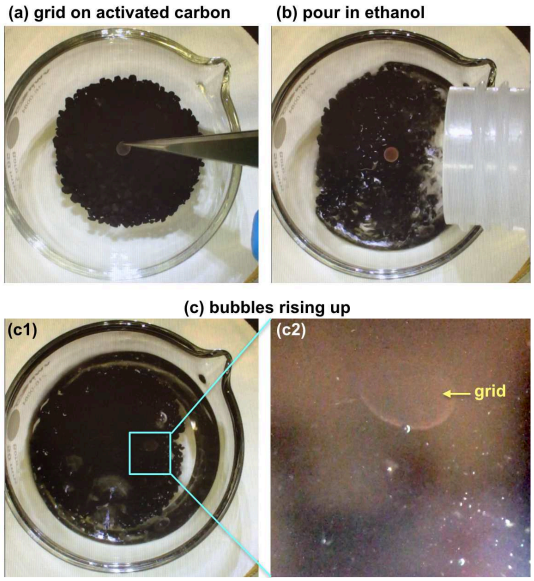

Figure 4 Step-by step demonstration of an alternative, more aggressive version of the grid cleaning method. (a) Place activated carbon into a container, and place a drop-cast TEM grid on top of the activated carbon. (b) Pour ethanol into the container until all the activated carbon is covered. (c1-2) A high density of bubbles rises up in the container, wait for a few minutes and then take out the grid and let it dry on a clean filter paper. The spots with bright contrast in (c2) are bubbles.

4. Discussion: mechanism and applications

To investigate the influence of ethanol and activated carbon in this method, we performed control experiments using different time, different solvents, and without using activated carbon.

	Procedure	Result
Method proposed in this work	Activated carbon + ethanol Submerge TEM grids for 10 min	Effective removal of contamination
Control experiment 01	Activated carbon + ethanol Submerge TEM grids for 2 or 24 hours	Effective removal of contamination But not better than 10 min
Control experiment 02	Activated carbon + ethanol After 15 min, submerge TEM grids	No removal of contamination
Control experiment 03	Ethanol Submerge TEM grids for 10 min, 2 hours	No removal of contamination
Control experiment 04	Flowing ethanol (100 rpm, 500 rpm) Submerge TEM grids for 10 min	No removal of contamination NPs agglomeration
Control experiment 05	Activated carbon + hexane Submerge TEM grids for 10 min	No removal of contamination
Control experiment 06	Activated carbon + methanol Submerge TEM grids for 10 min	Effective removal of contamination But methanol is toxic
Control experiment 07	Activated carbon + isopropanol Submerge TEM grids for 10 min	Reduction of contamination But less effective than ethanol

Table 2. Control experiments demonstrate that it is essential to use the combination of activated carbon and non-solvent.

As already mentioned in section 3, we also submerged TEM grids in activated carbon + ethanol for longer periods including 2 and 24 hours (Control experiment 01 in Table 2). Although both treatments cleaned the grids, they did not show obvious improvements in

comparison to submerging the grid for 10 min, which is roughly the period when bubbles arise. We also performed control experiment 02 (Table 2) in the following manner: after pouring ethanol onto activated carbon, we waited 15 min until no more bubbles appeared, then we submerged a drop-cast TEM grid into the mixture of activated carbon and ethanol. However, electron microscopy investigation did not show any removal of the contamination problem for this TEM grid. Both observations demonstrate the importance of the bubbles during the cleaning methodology.

Next, we consider the role of the solvent in our method. In general there are two fundamental mechanisms to stabilize the dispersion of colloidal NPs in solvents (control over NPs-aggregation): electrostatic and steric [1]. For the electrostatic mechanism, colloidal NPs are stabilized by adsorption of charged species to their surface by using solvents with high dielectric constant such as formamide. This mechanism is not applied here. For the steric mechanism, colloidal NPs are stabilized by surface-coating of organic ligands (usually hydrocarbon chains). Then, a good solvent brings a negative chain-solvent mixing energy hence inducing NPs to repel each other and stabilize the dispersion of NPs. For NPs capped by hydrocarbon ligands, typical good solvents are nonpolar liquids such as hexane and toluene. On the other hand, a non-solvent (also referred to as anti-solvent) brings positive chain-solvent mixing energy inducing contraction of ligand chains and aggregation of dispersed NPs. For NPs capped by hydrocarbon ligands, typical non-solvents are polar liquids such as ethanol, methanol and acetone.

To purify NPs when they are in solution, a precipitation and redissolution method is often used. Non-solvents are used in the precipitation step to increase the polarity of the solvent mixture, therefore the excess ligands in the supernatant can be decanted away after the centrifugation of NPs. Hence, for our CuAg NPs, a mixture of ethanol and 2-propanol as a non-solvent was employed for the centrifugation. Then, good solvents are used as re-dispersion solvent for the precipitated NPs to achieve good dispersion. In our experiment, hexane was employed as a good solvent for the redissolution step. These processes can be repeated several times to improve the purity of the NPs by removing the excess ligands in the solvent [22]. However, it should be noted that NPs might irreversibly aggregate after too many repetitions of the purification processes, and they cannot be redispersed in their good solvents anymore. Therefore, a tiny amount of fresh ligands are sometimes added into the colloidal NP dispersions during the purification process or even during storage, in order to keep the NPs stable without aggregation before structural and compositional analysis by electron microscopy. In other words, excess ligands might play an important role to prevent NPs from aggregation. In order to investigate the structure of individual NPs in TEM, overdoing the purification process should be avoided. However, when the excess ligands cannot be effectively removed from the NP dispersion prior to drop-casting on TEM grids, they become a major source of carbon contamination during electron microscopy investigation, thus impeding structural and compositional analyses at single particle and atomic scales.

Our method provides an alternative approach to wash the excess ligands for TEM investigation, in which the excess ligands are removed after drop-casting NPs on TEM grids and the over-purification of NPs can be avoided. When the drop-cast TEM grids

were submerged into ethanol, the excess ligands on TEM grids are likely to detach from the grids. Then, the excess ligands would contract and aggregate, similar to what happens in the NPs purification process. However, the situation for the ligands binding on the surface of the NPs is different. After the synthesis and purification processes, the surface of the NPs is coordinated primarily by the TDPA ligands [23]. The binding of the ligands to the NP surfaces has been confirmed by a variety of spectroscopic techniques [24], and is likely to be stronger than the binding of the ligands to the TEM grids. It is possible that the surface ligands might detach from the NP cores, which might be a dynamic process involving both attachment and detaching. However when the density of dispersed NPs is low enough that they are not overlapping or adjacent, the aggregation of NPs is not observed after submerging the TEM grids in activated carbon + ethanol.

To evaluate if the non-solvent by itself is enough to clean the TEM grids without activated carbon, we performed control experiment 03 by submerging TEM grids in ethanol without activated carbon for 10 min and 2 hours. The results show that no cleaning effect was observed. Since in the control experiments 01-02 we demonstrated that the bubbling period is essential for cleaning the TEM grid, we therefore hypothesized that the lack of ethanol flow in control experiment 03 might result in the inability to carry the excess ligands away from the TEM grids. Therefore, we performed control experiment 04 by submerging TEM grids in flowing ethanol. Hereby, a magnetic stirring bar in a container was used to flow the ethanol for 10 min (see supplementary movie 04 and Fig. S4). A slow speed setting of 100 revolutions per minute (rpm) and a faster speed setting of 500 rpm were applied and the results are similar: no reduction of the contamination was observed, and moreover, NPs agglomerated together (Fig. S5). Clearly, control experiment 04 shows that flowing ethanol alone does not result in cleaning the ligand contamination. Therefore, we conclude that it is essential to involve activated carbon in this cleaning method.

Based on the information above, a mechanism for our approach is proposed and demonstrated by the sketches in Fig. 5. Due to the porous features of the activated carbon (Fig. S6), air inside the pores of activated carbon will escape when liquids such as ethanol are poured into a container of activated carbon. This results in air bubbles (Fig. 5(a)) that go through and around a TEM grid when it is put into the ethanol (Fig. 5(b)). Then the excess ligands detach from the TEM grid and are carried along by the ethanol flow caused by the air bubbles. Next, when the excess ligands pass an activated carbon grain, they are trapped by the activated carbon (Fig. 5(c)). Moreover, the excess ligands in ethanol could contract and aggregate, enabling them to sink easily and subsequently be trapped by the activated carbon present at the bottom of the container. When there is no activated carbon but only flowing ethanol, excess ligands might also detach from the TEM grids, however they are likely to adhere back to the surface of TEM grids since there are no other adsorbent material in the liquid. This explains why we need both activated carbon and non-solvent. This also explains why submerging the TEM grid after the “bubbling” period did not reduce the contamination.

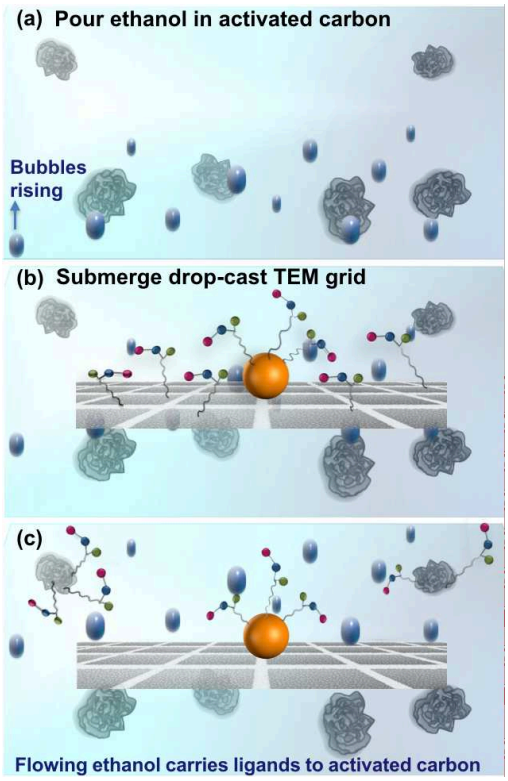

Figure 5 Illustrations showing the mechanism of the cleaning method. (a) When ethanol is poured into a container of activated carbon, air inside the pores of activated carbon escapes, resulting in air bubbles (blue balls). (b) A TEM grid with drop-cast NPs (orange balls) is submerged into ethanol and bubbles go through and around it. (c) The excess ligands detach from the TEM grid and are carried along by the ethanol flow caused by the air bubbles, and finally trapped by the activated carbon. The red-blue-green chains indicate organic ligands.

If the proposed mechanism is correct, the cleaning method should *not* work when good solvents are applied, while should work when non-solvents are used. Therefore, we investigated the use of a good solvent, hexane, as the solvent in the cleaning method (control experiment 05 in Table 2). The result shows no improvement in the contamination of the TEM grid. We also investigated the use of methanol and isopropanol as the non-solvent (control experiments 06 and 07 in Table 2). The results show that methanol removed the contamination similarly to the use of ethanol. However, since methanol is more toxic than ethanol, ethanol is preferred in our experiments. Isopropanol reduced the contamination, however a slight residue of ligand contamination was observed. The reason that isopropanol is not as effective as ethanol at cleaning the ligands might be due to its lower polarity: the relative polarities of isopropanol, ethanol and methanol are 0.548, 0.654 and 0.762 [25]. Although water has a high polarity (the relative polarity of water is 1.000), it is not appropriate to be used in our method. As demonstrated in Fig. S7, after pouring water into activated carbon, a thin layer of tiny carbon pieces floated on the surface of water, which are likely to attach to the TEM grids.

We have applied this method on different types of TEM grids and achieved successful cleaning effects, including TEM grids with continuous ultrathin carbon film shown in Fig.

3, with holey carbon film shown in Fig. S1, with graphene film as well as SiN film shown in Fig. S8.

Beside the CuAg and CuSn NPs with TDPA as capping ligands, this method has also shown effective decontamination on TEM grids for several other materials including metal NPs such as Au NPs with hexadecyltrimethylammonium bromide (CTAB) prepared via the method in [26]; semiconductor NPs such as InZnP/ZnMgSe quantum dots with oleylamine prepared via the method in [27] and CdSe/CdS with oleate prepared via the method in [28], PbS nanosheets with oleic acid, oleylamine and thiocyanate via the method in [29]; one-dimensional nanomaterials such as carbon nanotubes with iohexol prepared via the method in [30] and two-dimensional materials such as graphene with hydrocarbon contamination. Further improvement of our method is still needed for atmosphere-sensitive materials such as hybrid perovskites. The approach also requires further development for grids that contain very high densities of NPs such as self-assembled NPs, as the NPs might agglomerate during the process. There are several ways to further improve the method: by optimizing the time the grid is submerged in the solution, by exploring the use of different types of non-solvents, and exploring the use of different environments such as inert environments.

5. Conclusions:

To remove the unwanted effect of contamination during electron microscopy investigations of NPs surrounded by ligands, an effective and facile method has been developed to clean the drop-cast TEM grids. A combination of activated carbon and non-solvent such as ethanol is hereby used. By performing and comparing control experiments, a mechanism for the approach is proposed: pouring non-solvent liquid into activated carbon pushes the air to escape from the high density of pores in activated carbon, causing bubbles and hence a rapid flow of the non-solvent. Excess ligands detach from the TEM grids, and are trapped by activated carbon. In this manner the ligands on TEM grids are effectively reduced and hence atomic resolution imaging and spectroscopy such as EDX and EELS become feasible. Depending on the type and density of the NPs, several conditions can be adjusted to optimize the cleaning parameters. This facile route does not require a dedicated experimental set-up and can be widely applied for different nanomaterials that suffer from the ligand-induced contamination problem.

Author contribution:

CL developed the method and wrote the paper. CL and APT tested this method on different materials. CL and DW performed the control experiments. APT checked activated carbon with tomography. DC and KVD supplied the CuAg and CuSn NPs samples, respectively. TB and SB conducted the project.

Acknowledgement:

This research was funded by the University Antwerp GOA project (ID 33928). DW acknowledges an Individual Fellowship funded by the Marie Sklodowska-Curie Actions (MSCA) in Horizon 2020 program (grant 894254 SuprAtom).

Reference:

[1] M.A. Boles, D. Ling, T. Hyeon, D.V. Talapin, The surface science of nanocrystals, Nat. Mater. 15 (2016) 141–153. doi:10.1038/nmat4578.

[2] A. Heuer-Jungemann, N. Feliu, I. Bakaimi, M. Hamaly, A. Alkilany, I. Chakraborty, et al., The Role of Ligands in the Chemical Synthesis and Applications of Inorganic Nanoparticles, Chem. Rev. 119 (2019) 4819–4880. doi:10.1021/acs.chemrev.8b00733.

[3] S. Horiuchi, T. Hanada, M. Ebisawa, Y. Matsuda, M. Kobayashi, A. Takahara, Contamination-Free Transmission Electron Microscopy for High-Resolution Carbon Elemental Mapping of Polymers, ACS Nano. 3 (2009) 1297–1304. doi:10.1021/nn9001598.

[4] O. Dyck, S. Kim, S.V. Kalinin, S. Jesse, Mitigating e-beam-induced hydrocarbon deposition on graphene for atomic-scale scanning transmission electron microscopy studies, Journal of Vacuum Science & Technology B, Nanotechnology and Microelectronics: Materials, Processing, Measurement, and Phenomena. 36 (2018) 011801_1–7. doi:10.1116/1.5003034.

[5] M. Huth, F. Porrati, C. Schwalb, M. Winhold, R. Sachser, M. Dukic, et al., Focused electron beam induced deposition: A perspective, Beilstein J. Nanotechnol. 3 (2012) 597–619. doi:10.3762/bjnano.3.70.

[6] W.F. van Dorp, C.W. Hagen, A critical literature review of focused electron beam induced deposition, J. Appl. Phys. 104 (2008) 081301–43. doi:10.1063/1.2977587.

[7] D.R.G. Mitchell, Contamination mitigation strategies for scanning transmission electron microscopy, Micron. 73 (2015) 36–46. doi:10.1016/j.micron.2015.03.013.

[8] C.M. McGilvery, A.E. Goode, M.S.P. Shaffer, D.W. McComb, Contamination of holey/lacey carbon films in STEM, Micron. 43 (2012) 450–455. doi:10.1016/j.micron.2011.10.026.

[9] T.C. Isabell, P.E. Fischione, C. O'Keefe, M.U. Guruz, V.P. Dravid, Plasma Cleaning and Its Applications for Electron Microscopy, Microsc. Microanal. 5 (2002) 126–135. doi:10.1017/S1431927699000094.

[10] A.J.V. Griffiths, T. Walther, Quantification of carbon contamination under electron beam irradiation in a scanning transmission electron microscope and its suppression by plasma cleaning, J. Phys.: Conf. Ser. 241 (2010) 012017_1–4. doi:10.1088/1742-6596/241/1/012017.

[11] N.J. Zaluzec, B.J. Kestel, D. Henriks, Reactive gas plasma specimen processing for use in microanalysis and imaging in analytical electron microscopy, in: Microsc. Microanal, 1997: pp. CONF–970834–26. https://www.osti.gov/biblio/537241.

[12] R.F. Egerton, P. Li, M. Malac, Radiation damage in the TEM and SEM, Micron. 35 (2004) 399–409. doi:10.1016/j.micron.2004.02.003.

[13] G. Algara-Siller, O. Lehtinen, A. Turchanin, U. Kaiser, Dry-cleaning of graphene, Appl. Phys. Lett. 104 (2014) 153115_1–5. doi:10.1063/1.4871997.

[14] J.J. Hren, Barriers to AEM: Contamination and Etching, in: Principles of Analytical Electron Microscopy, Springer, Boston, MA, Boston, MA, 1986: pp. 353–374. doi:10.1007/978-1-4899-2037-9_10.

[15] C. Soong, P. Woo, D. Hoyle, Contamination Cleaning of TEM/SEM Samples with the ZONE Cleaner, Micros. Today. 20 (2012) 44–48. doi:10.1017/S1551929512000752.

[16] D. Hoyle, M. Malac, M. Trudeau, P. Woo, UV Treatment of TEM/STEM Samples for Reduced Hydrocarbon Contamination, Microsc. Microanal. 17 (2011) 1026–1027. doi:10.1017/S1431927611006003.

[17] G.T. Leuthner, S. Hummel, C. Mangler, T.J. Pennycook, T. Susi, J.C. Meyer, et al., Scanning transmission electron microscopy under controlled low-pressure atmospheres,

Ultramicroscopy. 203 (2019) 76–81. doi:10.1016/j.ultramic.2019.02.002.
[18] C. Li, J. Poplawsky, Y. Yan, S.J. Pennycook, Understanding individual defects in CdTe thin-film solar cells via STEM: From atomic structure to electrical activity, Mater. Sci. Semicond. Process. 65 (2017) 64–76. doi:10.1016/j.mssp.2016.06.017.
[19] C. Li, Y.-Y. Zhang, T.J. Pennycook, Y. Wu, A.R. Lupini, N. Paudel, et al., Column-by-column observation of dislocation motion in CdTe: Dynamic scanning transmission electron microscopy, Appl. Phys. Lett. 109 (2016) 143107–6. doi:10.1063/1.4963765.
[20] W.T. Osowiecki, X. Ye, P. Satish, K.C. Bustillo, E.L. Clark, A.P. Alivisatos, Tailoring Morphology of Cu–Ag Nanocrescents and Core–Shell Nanocrystals Guided by a Thermodynamic Model, J. Am. Chem. Soc. 140 (2018) 8569–8577. doi:10.1021/jacs.8b04558.
[21] Q. Li, J. Fu, W. Zhu, Z. Chen, B. Shen, L. Wu, et al., Tuning Sn-Catalysis for Electrochemical Reduction of CO_2 to CO via the Core/Shell Cu/SnO_2 Structure, J. Am. Chem. Soc. 139 (2017) 4290–4293. doi:10.1021/jacs.7b00261.
[22] Y. Shen, M.Y. Gee, A.B. Greytak, Purification technologies for colloidal nanocrystals, Chem. Commun. 53 (2017) 827–841. doi:10.1039/C6CC07998A.
[23] A. Glaria, J. Cure, K. Piettre, Y. Coppel, C.-O. Turrin, B. Chaudret, et al., Deciphering Ligands' Interaction with Cu and Cu_2O Nanocrystal Surfaces by NMR Solution Tools, Chem. Eur. J. 21 (2014) 1169–1178. doi:10.1002/chem.201403835.
[24] J.R. Pankhurst, P. Iyengar, A. Loiudice, M. Mensi, R. Buonsanti, Metal–ligand bond strength determines the fate of organic ligands on the catalyst surface during the electrochemical CO_2 reduction reaction, Chemical Science. 11 (2020) 9296–9302. doi:10.1039/D0SC03061A.
[25] C. Reichardt, Solvents and Solvent Effects in Organic Chemistry, 1st ed., Wiley, 2004. doi:10.1002/3527601791.
[26] G. González-Rubio, J. Mosquera, V. Kumar, A. Pedrazo-Tardajos, P. Llombart, D.M. Solís, et al., Micelle-directed chiral seeded growth on anisotropic gold nanocrystals, Science. 368 (2020) 1472–1477. doi:10.1126/science.aba0980.
[27] J.T. Mulder, N. Kirkwood, L. De Trizio, C. Li, S. Bals, L. Manna, et al., Developing Lattice Matched ZnMgSe Shells on InZnP Quantum Dots for Phosphor Applications, ACS Appl. Nano Mater. 3 (2020) 3859–3867. doi:10.1021/acsanm.0c00583.
[28] J. Leemans, S. Singh, C. Li, S. Ten Brinck, S. Bals, I. Infante, et al., Near-Edge Ligand Stripping and Robust Radiative Exciton Recombination in CdSe/CdS Core/Crown Nanoplatelets, J. Phys. Chem. Lett. 11 (2020) 3339–3344. doi:10.1021/acs.jpclett.0c00870.
[29] Q.A. Akkerman, B. Martín-García, J. Buha, G. Almeida, S. Toso, S. Marras, et al., Ultrathin Orthorhombic PbS Nanosheets, Chem. Mater. 31 (2019) 8145–8153. doi:10.1021/acs.chemmater.9b02914.
[30] S. Cambré, P. Muyshondt, R. Federicci, W. Wenseleers, Chirality-dependent densities of carbon nanotubes by in situ 2D fluorescence-excitation and Raman characterisation in a density gradient after ultracentrifugation, Nanoscale. 7 (2015) 20015–20024. doi:10.1039/C5NR06020F.